Controllable synthesis of high surface area Nb_2O_5 nanowires by polyamide

Zhenwei Zhang[1] ✉, *Jintao Zhang*[1], *Yue Chuanjun*[1], *Hu Jianheng*[2], *Zheng Shifu*[2]

[1]*School of Mathematical Sciences and Chemical Engineering, Changzhou Institute of Technology, Changzhou 213022, People's Republic of China*
[2]*School of Chemical Engineering, Changzhou University, Changzhou 213164, People's Republic of China*
✉ *E-mail: qianyangrun@163.com*

Published in Micro & Nano Letters; Received on 7th March 2017; Revised on 1st August 2017; Accepted on 1st September 2017

A high surface area Nb_2O_5 nanowire material was synthesised by the soft chemical method using polyamide (Pebax) as a structure direct agent and isopropanol as a solvent. The crystal size and BET surface area of Nb_2O_5 were tuned by the quantity of Pebax. The surface area can reach up to 402 m^2 g^{-1}, which is higher than the reported value in the literature. Adsorption properties and photocatalyst properties were tested using methylene blue (MB), neural red (NR), Rhodamine B (RhB), and methyl orange (MO). The results show that MB and NR exhibit a good adsorption performance, the molecular structures of the dyes have a tricyclic aromatic ring and several amine groups can improve their adsorption properties. In a photocatalyst reaction, Nb_2O_5 has a selective activity for dye degradation. After 2 h of ultraviolet irradiation, the degradation rate of MB is about 91.9%, but the NR was degraded little.

1. Introduction: Niobium oxide (Nb_2O_5) is a special kind of semiconductor metal oxide, which is stable under acidic conditions [1]. It is widely applied in chemical sensors [2], catalysis [3], electrochemistry [4] and photocatalytic reactions [5]. In the present work, the different morphologies of Nb_2O_5 were showing different physical and chemical properties [6]. Nb_2O_5 nanosheets exhibit excellent properties in a supercapacitor [7].

One-dimensional Nb_2O_5 materials, nanorods and nanowires, also having special physicochemical properties have been reported in recent reports. George *et al*. [8] used niobium ethoxide as a raw material to prepare Nb_2O_5 nanorods at 500°C. Li *et al*. [9] reported that single-crystal Nb_2O_5 nanorods were prepared by a localised molten salt method. Zhou *et al*. [10] used niobium fluoride and ammonia in water/ethanol mixed solvent to prepare highly crystalline TT-Nb_2O_5 nanorods, the aspect ratio of the nanorods was well controlled by the water/ethanol ratio. Above all, nanorods prepared by these methods exhibited good morphology and good crystallinity, but the raw material is expensive, the specific surface area and catalytic performance were low.

Akihiko [11] used ammonium niobium oxalate as a raw material and trioctylamine as a guide to prepare Nb_2O_5 nanowires with a width of 30–50 nm. Viet *et al*. [12] used gel electrospinning technology to produce TT-Nb_2O_5 nanofibres, and the average width was about 160 nm. Lim and Choi [13] invented a new method for the preparation of Nb_2O_5 nanowires. The Nb_2O_5 prepared by these methods exhibited high crystallinity and high energy consumption, and the surface acidity of Nb_2O_5 disappeared without high catalytic activity. Jana and Rioux [14] used $NbCl_5$ as the precursor to prepare Nb_2O_5 nanowires in oleic acid. The nanowire morphology of Nb_2O_5 was well controlled and the synthesis process was simple. However, the size of the nanomaterial was uncontrollable, and its catalytic performance was not clear and its specific surface area was also low.

The template method was also used to synthesise high specific surface area Nb_2O_5 nanomaterials by P123, CTAB, F127, etc. [15]. The highest specific surface area of Nb_2O_5 prepared by P123 can reach up to 343 m^2 g^{-1} [16]. In addition, niobium oxalate reacted with hydrogen peroxide [17] to form Nb_2O_5 nanomaterial owing to the high surface area of about 327 m^2 g^{-1}, but the Nb_2O_5 exhibited an amorphous structure. Additionally, P123, P85, CTAB and other templates are difficult to recovery, some even decomposed in the synthesis process. Moreover, the template method can mainly produce mesoporous structures but not nanorods or nanowires.

In this Letter, a new structure direct agent polyamide (Pebax2533) was described to synthesise Nb_2O_5 nanowires and nanofibres by the hydrothermal method (see Fig. 1). The Pebax structure exhibits stability, strong acid or alkali resistivity [18], solubility in isopropyl alcohol and recyclability. In solution, Pebax exhibited higher viscosity, and the nanocrystalline particles in the solvent system cannot easily aggregate [19]. Additionally, the dodecyl amide chains in the polymer can form hydrogen bonds between each other especially under acid conditions, the structure is fixed as the polymer 'hard segments' [20], 1,4-butanediol chains in the structure are changeable, known as 'flexible segments', these extraordinary properties make Nb_2O_5 produce porous nanofibres. The specific surface area of the prepared Nb_2O_5 can reach up to 402 m^2 g^{-1}, which is higher than that reported in the literature. In addition, Nb_2O_5 having a semiconducting property can be applied to the degradation of contaminants [21]. Adsorption and degradation of methylene blue (MB), methyl orange (MO), neutral red (NR) and rhodamine B (RhB) were studied to investigate the properties of high specific surface area Nb_2O_5 nanowires.

2. Experimental details

2.1. Experimental materials: Isopropyl alcohol (AR, > 99%), MB (AR, > 98%), MO (AR, > 98%), NR (AR, > 98%), and RhB (AR, > 98%) were purchased from Shanghai Lingfeng Chemical Reagent Co. Ltd. Deionised water was prepared from the OKP equipment which was purchased from Shanghai Lakecore Company. Ammonium niobium oxalate ($NH_4[NbO(C_2O_4)_2(H_2O)_2]\cdot nH_2O$) was purchased from Qiandao Ruike Chemical Company. Polyamide (Pebax2533) was purchased from ARKEMA Firm.

2.2. Synthesis of high specific surface area Nb_2O_5 nanofibres and nanowires: Pebax (20 g) was dissolved in 100 ml of isopropanol and stirred at 80°C overnight. 40 ml niobium oxalate saturated aqueous solution was poured into the above Pebax solution, and stirred well. The mixture was poured into a polytetrafluoroethylene-lined stainless steel reaction vessel and hydrothermally treated under 180°C for 7 days to get a white precipitate. Then washed the precipitate several times using isopropyl alcohol at 80°C, the white solid dried in an oven at 70°C. The as-prepared Nb_2O_5 was named N-1. Change the amount of Pebax as follow: 10 g or 5 g, respectively, to prepare Nb_2O_5 with different specific surface areas, and make other

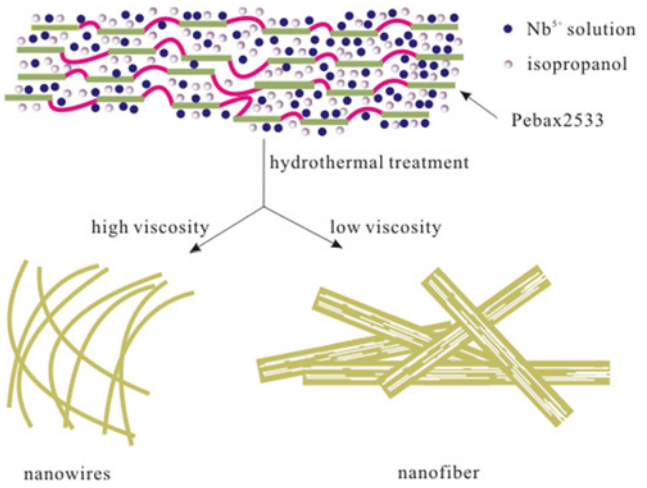

Fig. 1 *Schematic approach for synthesis of Nb_2O_5 nanowires*

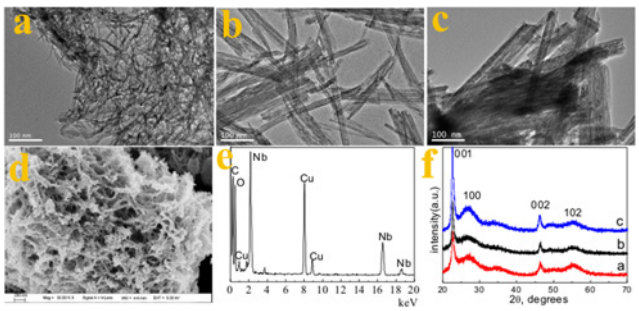

Fig. 2 *TEM (a, b, c), SEM (d), EDS (e) and XRD (f) analysis of Nb_2O_5*
a N-1
b N-2
c N-3
d N-1
e N-1
f a N-1; b N-1; c N-3

conditions the same, the Nb_2O_5 prepared by 10 g Pebax was named N-2, and the Nb_2O_5 prepared by 5 g Pebax was named N-3.

2.3. Adsorption performance assessment: The adsorption performance of Nb_2O_5 nanomaterials was tested as follows: the aqueous solution of MB, NR, RhB and MO with different concentrations and different pH values was prepared as per the simulation of contaminants. Under dark conditions, 10 mg of Nb_2O_5 were dispersed in 100 mL aqueous solution. The sample mixture was extracted at 1 min intervals and then centrifuged at 8000 rpm for 2 min to remove the solid. The supernatant was measured by ultraviolet (UV) spectroscopy to determine the residual concentration of the contaminants. The wavelength range was set as follows: 450–750 (MB), 200 (NR), 440–600 (RhB), and 200–600 nm (MO), respectively.

2.4. Photocatalytic performance assessment: 50 mg of Nb_2O_5 catalyst were dissolved in 50 mL of 40 mg L^{-1} aqueous contaminant solution. The mixture was stirred in the dark for 35 min to make an adsorption–desorption equilibrium. The photocatalysis was performed at room temperature using a Luzchem photocatalytic reactor with a wavelength of 350 nm and a power of 0.3 mW cm^{-2}. Reaction time was 2 h. Take a sample every 10 min and then centrifuge at 8000 rpm for 5 min to remove solids. The supernatant was measured by UV spectroscopy to determine the residual concentration of the contaminants.

2.5. Characterisation: X-ray powder diffraction (XRD) patterns were recorded on a D/MAX 2500/PC powder diffractometer (Rigaku) using a CuKα radiation source operated at 40 kV and 200 mA from 5° to 70° (in 2θ) with a scanning rate of 20° min^{-1}. X-ray photoelectron spectroscopy (XPS) was performed using a Thermo Scientific Escalab 250 instrument under ultrahigh vacuum conditions with a pressure close to 2×10^{-9} mbar. Transmission electron microscopy (TEM; JEOL JEM-2100) and energy-dispersive X-ray spectroscopy (EDS) were applied for the detailed microstructure and composition information. The surface area and pore size distributions were measured by the surface area and pore size analyser (Autosorb-iQ2-MP). The concentration of contaminants was determined by an ultraviolet and visible spectrum instrument (UV-759S).

3. Results and discussion

3.1. Characterisation of Nb_2O_5: TEM characterisation can analyse the morphology of nanomaterials. In Fig. 2*a* the synthesised Nb_2O_5 (N-1) exhibits a wire-like morphology and the width of nanowire was about 8 nm. Scanning electron microscopy (SEM) analysis result was (Fig. 2*d*) in accordance with TEM images that the morphology was linear and nanowires were grouped into follower-like nanostructure. Nb_2O_5 crystal size becomes larger when less Pebax was used. In Fig. 2*b*, the diameter of the wire N-2 was about 20 nm and in Fig. 2*c*, N-3 nanowires exhibited nanofibre morphology using the lowest Pebax. The elemental composition of Nb_2O_5 was characterised by elemental analysis (EDS) of TEM (EDS) (Fig. 2*e*), and the elemental types are Nb and O (Cu and O are copper network elements). Nb atomic percentage is 11.58%, O atomic percentage is 29.29%, so the Nb: O atomic ratio is about 1:2.5 and Nb_2O_5 structural formula values are basically the same. From the XRD data, the intensity of the (001) and (002) crystal planes of Nb_2O_5 at 22.6° and 46.3° is high, and the intensity of the (100) and (102) planes at 26.7 and 55.4 is weak, indicating that Nb_2O_5 crystals exhibited a special morphology. Consistent with the literature values [22]. The size of Nb_2O_5 crystal grains was adjusted by tuning the amount of template Pebax. From the XRD pattern (Fig. 2*f*), the intensity of (001) crystal peaks of the three samples is different. The larger the Pebax template dose, the smaller the peak intensity of the crystal face. The Debye–Scherrer formula shows that under the largest amount of Pebax, the smallest crystal size Nb_2O_5 formed. This work is similar to the mechanism described in the literature [19]. The Pebax block copolymer consists of a lipophilic Polyamide (PA) fragment (nylon-12) and a hydrophilic polyether (PE) (poly-1,4-butanediol) fragment. The Pebax chain in the solvent blocks the whole system into numerous water and oil phases due to the hydro-lipophilic effect in the hydrothermal environment. The larger the amount of Pebax, the smaller the volume of the solvent phase blocked, niobium oxalate in the aqueous phase is decomposed into Nb_2O_5, the oil phase and Pebax chain played barrier roles. Another reason is more Pebax form a higher kinematic viscosity condition causing lower collision probability between nanoparticles, giving smaller Nb_2O_5 crystal size.

To further clarify the covalent value of niobium oxides, XPS analysis was used. The XPS spectrum of the as-prepared N-1 is shown in Fig. 3. Nb, O, and C elements are shown to be consistent with the EDS results. Carbon indicates that a small amount of organic residue on the surface of Nb_2O_5 is not washed off by isopropanol. Fig. 3 shows the binding energies of Nb 3d, Nb $3d_{5/2}$ and Nb $3d_{3/2}$ are 207.8 and 210.5 eV, respectively, and the result was consistent with the literature [23], Nb atomic percentage is about 20.06%, O atomic percentage is about 52.07%, and the results are in agreement with those of elemental analysis.

3.2. Regulate the specific surface area: In the experimental process, the size and specific surface area of Nb_2O_5 nanowires can be

doi: 10.1049/mnl.2017.0104

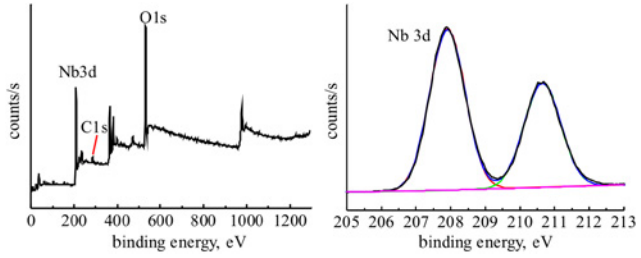

Fig. 3 *XPS analysis of N-1*

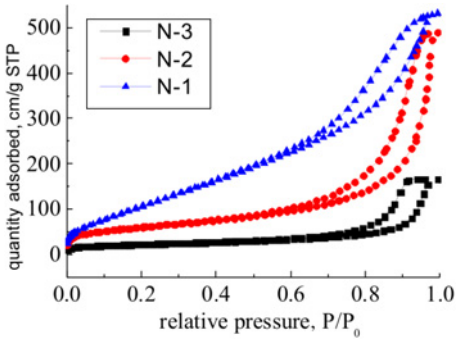

Fig. 4 *N_2 adsorption–desorption determination of N-1, N-2, N-3*

controlled by adjusting the amount of Pebax. Fig. 4 shows the N_2 adsorption–desorption data of Nb_2O_5. When using 20 g Pebax, the specific area of Nb_2O_5 can reach up to 402 m^2 g^{-1}, which is higher than the value of 327 m^2 g^{-1} given in the literature. In addition, it was found that when the amount of Pebax was increased to 25 g or more, Brunauer-Emmett-Teller specific surface area (BET) was decreased. This is because Nb_2O_5 particles are too small, too many polymers, wrapped on the Nb_2O_5 surface are more difficult to remove. The three types of hysteresis loops are all H4, indicating that the structure of the material N-1 has slit pores, which is consistent with the characterisation data of TEM and SEM. It is proved that Nb_2O_5 has a linear or strip structure. When the amount of Pebax is 10 g, the specific surface area of Nb_2O_5 N-2 is 213 m^2 g^{-1}. When the amount of Pebax was 5 g, the specific surface area was 73 m^2 g^{-1}. When the amount of Pebax is reduced, the solvent volume of the water phase and oil phase separated by the Pebax chain barrier becomes larger, and Nb_2O_5 particles are decomposed in the water phase, and the corresponding specific surface area becomes smaller.

4. Application of Nb_2O_5

4.1. Adsorption properties of Nb_2O_5: The adsorption properties of Nb_2O_5 are shown in Fig. 5 using four different contaminants: MB, NR, RhB and MO. N-1 (10 mg) was dissolved in 100 ml solution with a pigment concentration of 20 mg L^{-1} and the pH value was kept at 7. The adsorption of RhB and MO is almost zero, the adsorption of NR is about 0.18 mg mg^{-1}, and the adsorption of MB is about 0.17 mg mg^{-1}.

The adsorption mechanism can be explained from the molecular structures of contaminants. There are ternary polycyclic aromatic rings in NR and MB, but MO is azo compounds, RhB is the quaternary aromatic compound (Fig. 5*c*). These indicate that compounds with ternary polycyclic aromatic structures are easily adsorbed by Nb_2O_5. In addition, acid sites on the surface of Nb_2O_5 are easy to adsorb negative electron groups. The number of N atoms in the NR structure is more than that of MB, and the amino groups are favourable to be adsorbed by Nb_2O_5 [24]. A MB molecule has a quaternary nitrogen atom compared with the structure of NR causing a great influence on the molecular charge exhibiting a lower adsorption performance. NR molecules without a quaternary ammonium structure and N atoms are evenly distributed throughout the molecule due to the charge dispersed evenly to each atom exhibiting a higher adsorption performance.

4.2. Comparison of the adsorption properties of different BET on Nb_2O_5: Based on the above results, Nb_2O_5 exhibits good adsorption performance to MB and NR, so MB and NR are used as the target of a comparative experiment. The effects of the specific surface area of Nb_2O_5 on the adsorption performance were studied. N-1, N-2 and N-3 were added into 100 ml dye solution, respectively, the solution concentration was 20 mg L^{-1} and the pH value solution was 7.0. Fig. 6 shows the adsorption capacity of MB and the adsorption capacity of N-1 was about 0.17 mg mg^{-1}, and the adsorption–desorption equilibrium is reached after 12 min. The specific surface area of N-2 was 213 m^2 g^{-1}, and the adsorption capacity was 0.076 mg mg^{-1}. The N-3 has a specific surface area of 73 m^2 g^{-1} and its adsorption capacity was only about 0.01 mg mg^{-1}. This is proportional to the number of acidic sites of Nb_2O_5, the higher the specific surface area is more acidic sites exhibit higher adsorption. The adsorption performance of NR is the same as that of MB. The adsorption capacity of N-1 is 0.19 mg mg^{-1}, and the adsorption–desorption equilibrium is reached after 20 min. The N-2 adsorption capacity of 0.14 mg mg^{-1} is half more than MB. This indicates that the adsorption performance is related to the amino group in the NR molecule, the number of nitrogen atoms is more than MB, and the adsorption performance is improved.

4.3. Isothermal adsorption properties of contaminants at different concentrations: The adsorption properties of Nb_2O_5 to MB and NR under different concentrations were further investigated. 10 mg of N-1 were dissolved in different concentrations of the solution, respectively, and kept the pH value at 7.0. In Fig. 7, when MB concentration reached up to 80 mg L^{-1}, the adsorption of Nb_2O_5 reached near saturation, which was about 0.208 mg mg^{-1}. When the concentration of NR was 80 mg L^{-1}, the adsorption reached 0.23 mg mg^{-1}. The experimental results are consistent with the above analysis, the NR molecular structure

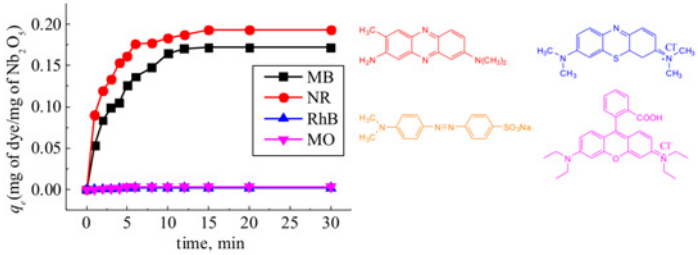

Fig. 5 *Adsorption performance of Nb_2O_5 in various kinds of dyes under different conditions*

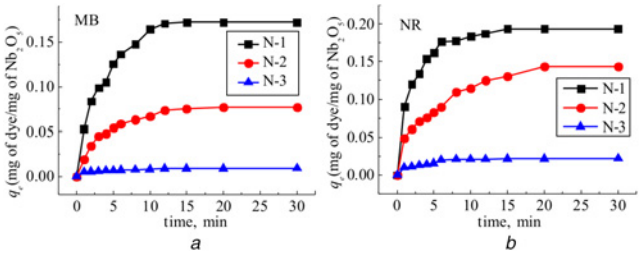

Fig. 6 *Adsorption performance of Nb_2O_5 owing different BET values to*
a MB
b NR

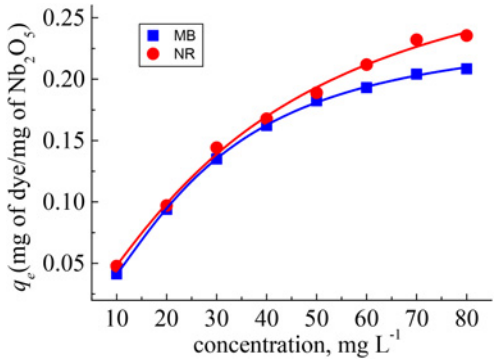

Fig. 7 *Adsorption properties of Nb_2O_5 under different concentrations of MB and NR*

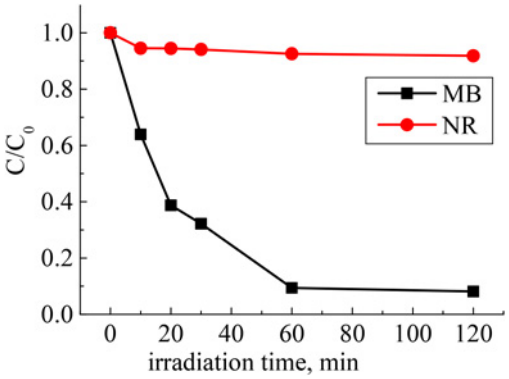

Fig. 8 *Degradation performance of Nb_2O_5*

has more number of nitrogen atoms than MB. The adsorption curves are in good agreement with Langmuir isothermal adsorption.

4.4. Photocatalytic activity of Nb_2O_5: The photocatalytic activity of Nb_2O_5 was evaluated using MB and NR as degradation targets. In this study, N-3 with a specific surface area of 73 $m^2\ g^{-1}$ was used to assess its photo-degradation properties. As shown in Fig. 8, the photodegradation concentration was about 20 mg L^{-1} and degradation test time was 2 h, and MB had a higher degradation of about 91.9%. The NR degradation rate is very low, only about 8.2%. The result showed that Nb_2O_5 could degrade contaminants selectively. Even Nb_2O_5 has the best adsorption performance for NR, but the degradability of NR is not good. According to the molecular structure, MB is easy for polarisation making the molecular structure unstable and easy for degradation.

5. Conclusion: The Nb_2O_5 nanomaterials with a high specific surface area were prepared by using polyamide compound as a structure direct agent and niobium oxalate as a niobium source. It has the highest specific surface area. The adsorption and degradation performances of Nb_2O_5 were tested by using MB, NR, RhB and MO. The adsorption of NR to Nb_2O_5 was the best, MB is the second best, and RhB and MO are poor. The MB degradation rate of Nb_2O_5 was 91.9%. The charge stability of the molecular structure significantly influenced the degradation rate.

6. Acknowledgments: This work has been supported by the Jiangsu Province Distinguished Professor Jiang Xingmao teacher funding (grant no. SCZ1211400001), the State Key Laboratory of Respiratory System, Changzhou Municipal Science and Technology Bureau (grant nos. CM20133005, 21503023, 21373034), the Changzhou Municipal Science and Technology Bureau, Changzhou City Key Laboratory of Respiratory Medicine (grant no. CM20133005), the Key Laboratory of Fine Petrochemical Industry and PAPD, Jiangsu University, Changzhou University, Jiangsu Province Key Laboratory of Advanced Catalytic Materials and Technology, Jiangsu Province, funded by the Changzhou University of Technology (YN1502, grant no. E3-6107-15 -026).

7 References

[1] Nakajima K., Baba Y., Noma R., *ET AL.*: 'Nb$_2$O$_5$·*n*H$_2$O as a heterogeneous catalyst with water-tolerant Lewis acid sites', *J. Am. Chem. Soc.*, 2011, **133**, (12), pp. 4224–4227
[2] Fiz R., Hernandez-Ramirez F., Fischer T., *ET AL.*: 'Synthesis, characterization, and humidity detection properties of Nb_2O_5 nanorods and SnO_2/Nb_2O_5 heterostructures', *J. Phys. Chem. C*, 2013, **117**, (19), pp. 10086–10094
[3] Tanabe K.: 'Catalytic application of niobium compounds', *Catal. Today*, 2003, **78**, (1–4), pp. 65–77
[4] Ou J.Z., Rani R.A., Ham M.-H., *ET AL.*: 'Elevated temperature anodized Nb_2O_5: a photoanode material with exceptionally large photoconversion efficiencies', *ACS Nano*, 2012, **6**, (5), pp. 4045–4053
[5] Zhao Y., Eley C., Hu J., *ET AL.*: 'Shape-dependent acidity and photocatalytic activity of Nb_2O_5 nanocrystals with an active Tt (001) surface', *Angew. Chem. Int. Ed.*, 2012, **51**, (16), pp. 3846–3849
[6] Tsang E., Zhou X., Ye L., *ET AL.*: 'Nanostructured Nb_2O_5 catalysts', 2012
[7] Li H., Zhu Y., Dong S., *ET AL.*: 'Self-assembled Nb_2O_5 nanosheets for high energy–high power sodium ion capacitors', *Chem. Mater.*, 2016, **28**, (16), pp. 5753–5760
[8] George P.P., Pol V.G., Gedanken A.: 'Synthesis and characterization of Nb_2O_5@C core-shell nanorods and Nb_2O_5 nanorods by reacting $Nb(OEt)_5$ via RAPET (reaction under autogenic pressure at elevated temperatures) technique', *Nanoscale Res. Lett.*, 2006, **2**, (1), p. 17
[9] Li L., Deng J., Yu R., *ET AL.*: 'Phase evolution in low-dimensional niobium oxide synthesized by a topochemical method', *Inorg. Chem.*, 2010, **49**, (4), pp. 1397–1403
[10] Zhou Y., Qiu Z., Lü M., *ET AL.*: 'Preparation and spectroscopic properties of Nb_2O_5 nanorods', *J. Lumin.*, 2008, **128**, (8), pp. 1369–1372
[11] Kenji S., Akihiko K.: 'Controlled synthesis of Tt phase niobium pentoxide nanowires showing enhanced photocatalytic properties', *Bull. Chem. Soc. Japan*, 2009, **82**, (8), pp. 1030–1034
[12] Viet A.L., Reddy M.V., Jose R., *ET AL.*: 'Nanostructured Nb_2O_5 polymorphs by electrospinning for rechargeable lithium batteries', *J. Phys. Chem. C*, 2010, **114**, (1), pp. 664–671
[13] Lim J.H., Choi J.: 'Formation of niobium oxide nanowires by thermal oxidation', *J. Ind. Eng. Chem.*, 2009, **15**, (6), pp. 860–864
[14] Jana S., Rioux R.M.: 'Seeded growth induced amorphous to crystalline transformation of niobium oxide nanostructures', *Nanoscale*, 2012, **4**, (5), pp. 1782–1788
[15] Ye L., Xie S., Yue B., *ET AL.*: 'Crystalline three-dimensional cubic mesoporous niobium oxide', *CrystEngComm*, 2010, **12**, (2), pp. 344–347
[16] Nakajima K., Fukui T., Kato H., *ET AL.*: 'Structure and acid catalysis of mesoporous Nb_2O_5·nH_2O', *Chem. Mater.*, 2010, **22**, (11), pp. 3332–3339
[17] Leite E.R., Vila C., Bettini J., *ET AL.*: 'Synthesis of niobia nanocrystals with controlled morphology', *J. Phys. Chem. B*, 2006, **110**, (37), pp. 18088–18090

doi: 10.1049/mnl.2017.0104

[18] Bernardo P., Jansen J.C., Bazzarelli F., *ET AL.*: 'Gas transport properties of Pebax®/room temperature ionic liquid Gel membranes', *Sep. Purif. Technol.*, 2012, **97**, pp. 73–82
[19] Jiang X., Brinker C.J.: 'Rigid templating of high surface-area, mesoporous, nanocrystalline rutile using a polyether block amide copolymer template', *Chem. Commun.*, 2010, **46**, (33), pp. 6123–6125
[20] Kamal T., Park S.-Y., Park J.-H., *ET AL.*: 'Structural evolution of poly (Ether-B-Amide12) elastomers during the uniaxial stretching: an in situ wide-angle X-ray scattering study', *Macromol. Res.*, 2012, **20**, (7), pp. 725–731
[21] Kominami H., Oki K., Kohno M., *ET AL.*: 'Novel solvothermal synthesis of niobium(V) oxide powders and their photocatalytic activity in aqueous suspensions', *J. Mater. Chem.*, 2001, **11**, (2), pp. 604–609
[22] Tamai K., Hosokawa S., Teramura K., *ET AL.*: 'Synthesis of niobium oxide nanoparticles with plate morphology utilizing solvothermal reaction and their performances for selective photooxidation', *Appl. Catal. B: Environmental*, 2016, **182**, pp. 469–475
[23] Ge S., Jia H., Zhao H., *ET AL.*: 'First observation of visible light photocatalytic activity of carbon modified Nb_2O_5 nanostructures', *J. Mater. Chem.*, 2010, **20**, (15), pp. 3052–3058
[24] Furukawa S., Ohno Y., Shishido T., *ET AL.*: 'Selective amine oxidation using Nb_2O_5 photocatalyst and O_2', *ACS Catal.*, 2011, **1**, (10), pp. 1150–1153